Acta Geodyn. Geomater., Vol. 20, No. 2 (210), 61–70, 2023
DOI: 10.13168/AGG.2023.0006
journal homepage: https://www.irsm.cas.cz/acta

ORIGINAL PAPER

TERRESTRIAL WATER STORAGE CHANGES OVER 25 GLOBAL RIVER BASINS EXTRACTED BY LOCAL MEAN DECOMPOSITION FROM GRACE MONTHLY GRAVITY FIELD SOLUTIONS

Changmin HUAN [1, 4], Fengwei WANG [2], Shijian ZHOU [3] * and Tieding LU [1, 4]

[1] *School of Surveying and Geoinformation Engineering, East China University of Technology, Nanchang, PR, China*
[2] *State Key Laboratory of Marine Geology, Tongji University, Shanghai, PR, China*
[3] *Nanchang Hangkong University, Nanchang, PR, China*
[4] *Key Laboratory of Mine Environmental Monitoring and Improving around Poyang Lake of Ministry of Natural Resources, East China University of Technology, Nanchang, PR, China*

**Corresponding author's e-mail:* 408608628@qq.com

ARTICLE INFO

Article history:
Received 23 May 2023
Accepted 13 June 2023
Available online 20 June 2023

Keywords:
GRACE
Terrestrial Water Storage Change
Local Mean Decomposition
Noise

ABSTRACT

The strong striping and high-frequency noise existed in Gravity Recovery and Climate Experiment (GRACE) solutions drowned the real geophysical signals, which need other signal extraction methods. Considering the advantages of local mean decomposition (LMD) in extracting geophysical signals from noisy time series, we adopt it to filter the noise and estimate the terrestrial water storage (TWS) changes over 25 global main river basins from the time series of 14-year (2002.04~2016.08) Release 06 (RL06) monthly gravity field models provided by Center for Space Research (CSR), together with the empirical mode decomposition (EMD) as a comparison. To evaluate the efficiency of eliminating noise by LMD and EMD, the ratios of the latitude weighted RMS over the land and ocean signals are adopted. The results show that all RMS ratios of land relative to ocean signals derived by LMD are higher than EMD with the mean values 3.4458 and 3.3302, respectively. Moreover, relative to the Global Land Data Assimilation System (GLDAS) Noah model, the extracted TWS changes by LMD approach have smaller root mean squared errors than EMD over 25 global river basins. Therefore, it is reasonable to conclude that LMD approach outperforms EMD in extracting TWS changes and filtering out the strong noise existed in GRACE monthly gravity field solutions.

1. 1 INTRODUCTION

GRACE satellites, launched in March 2002, provided the possibility to directly monitor the Earth's time-varying gravity field gradually and which is valuable to detect the large-scale changes such as surface land water, groundwater, glacier melting and ocean mass changes etc. (Chen et al., 2002; Wouters et al., 2014). Due to the limitation of GRACE satellite orbit, sensor error, aliasing of sampling frequency and other reasons, there exists strong noise in the obtained spherical harmonic (SH) coefficients models, especially the north-south striping (NSS) error, which make the geophysical signals drowned in strong noise (Yi and Sneeuw, 2022), therefore developing suitable signal extraction method is great valuable.

For the tough problem, many approaches were developed and adopted to reduce the strong noise of GRACE spherical harmonic coefficient models to better extract the geophysical signals. And, in order to better follow up work, several GRACE data release official agencies were launched. The new generation of GRACE observation data products: Mascon products which are provided by the Center for Space Research at University of Texas (CSR), NASA Jet Propulsion Laboratory (JPL) and Goddard Space Flight Center (GSFC). These Mascon products are solved in a couple of ways, which include the regularization methods for the monthly gravity field solutions (one type is the post-processing (Klees et al., 2008; Swenson and Wahr, 2011) and the other is solving along with the least-squares estimation (Chen et al., 2021; Zhong et al., 2023). Firstly, the commonly used Gaussian smoothing with a certain radius was proposed by Wahr et al. (1998), whose smoothing kernel function was constructed based on the degrees of SH coefficients. On the basis of Gaussian smoothing, Han et al. (2005) modified and developed the anisotropic Gaussian filtering algorithm. Besides, Fan filtering (Zhang et al., 2009) and Wiener filtering (Sasgen et al., 2007), were also proposed to filter noise and extract real geophysical signals. However, these above-mentioned filtering methods will certainly lead to the signal leakage during the filtering procedure for better reducing the NSS error to eliminate the correlation error between odd and even orders of the degree. In this contribution, the sliding window polynomial fitting de-correlation algorithm (Chambers and Bonin, 2012), PnMm approach

Cite this article as: Huan Ch, Wang F, Zhou S, Lu T: Terrestrial water storage changes over 25 global river basins extracted by local mean decomposition from GRACE Monthly Gravity Field solutions. Acta Geodyn. Geomater., 19, No. 2 (210), 61–70, 2023. DOI: 10.13168/AGG.2023.0006

(Chambers and Bonin, 2012; Chen et al., 2007), sliding variable window polynomial fitting de-correlation filtering algorithm (Duan et al., 2009) were proposed. A two-step (de-striping and Gauss based smoothing) process that take on account possible over smoothing results, introduces additional uncertainty, and error propagation, a low-pass spectral filtering algorithm is proposed (Yang et al., 2022).

Above these two introduced filtering types, other effectively signal extraction methods, such as statistical filter (Davis et al., 2008), independent component analysis filter (Guo et al., 2014), principal component analysis filter (Mu et al., 2014), multichannel singular spectral analysis (Wang et al., 2020; Shen et al., 2021), empirical mode decomposition (Huan et al., 2022; 2023), etc. Among these methods, EMD can adaptively extract the periodic components of different frequencies and amplitudes without need any prior information and parameters, however, it can be easily affected by the endpoint effect and needs more iterations. Compared with EMD approach, LMD has been effectively improved in terms of aliasing modes, endpoint effects, over enveloping and under-enveloping (Wang et al., 2010) etc., which has been widely used in various research fields such as GNSS signal processing (Qiu et al., 2020), natural gas pipeline leak aperture identification and location (Sun et al., 2016), processing of scalp electroencephalographic visual perception data (Smith, 2005) and in fault diagnosis of rotating machinery (Cheng et al., 2012), therefore we will adopt the LMD to extract the real geophysical signals from noisy GRACE gravity field solutions, and take EMD as the comparisons. The rest of this paper is organized as follows: Section 2 introduces the method and data used in this study, Section 3 analyzes the results from three aspects, Section 4 shows the summary of experiment results.

2. PROCESSING METHODS AND ADOPTED DATASETS

2.1. LOCAL MEAN DECOMPOSITION

Local mean decomposition (LMD) is a new spectral class analysis method proposed in recent years. And it is a new adaptive time-frequency analysis method, that can decompose the complex multi-component amplitude-modulation signal into a finite sum of single-component amplitude-modulation signals according to the characteristics of the signal itself, and then obtain the instantaneous frequency and instantaneous amplitude and combine them to obtain the complete time-frequency distribution of the original signal, therefore, it does not need prior information and it has a posteriori property. The adaptability of this method has a good effect in processing non-stationary and non-linear time series. The LMD method compared to the EMD method has some advantages, which are better than EMD method in suppressing end effect, reducing the number of iterations and preserving signal integrity, false component, over envelope and under envelope in practical application. According to the characteristics of the signal, LMD can decompose the complex multi-component time series into several components related to signal and noise. The procedures of LMD approach are as follows:

1. For the original time series $x(t)$, find out each local extreme point n_i, and calculate the average value of n_i and n_{i+1}:

$$m_i = (n_i + n_{i+1})/2 \tag{1}$$

2. Calculate local amplitude a_i:

$$a_i = |n_i - n_{i+1}|/2 \tag{2}$$

All local amplitudes a_i are extended in a straight line between t_i and t_{i+1} at the time of the corresponding extreme point, and the extended straight line is smoothed by the moving average method to obtain the envelope estimates $a_{11}(t)$.

3. The local mean value function $m_{11}(t)$ is separated from the original series $x(t)$:

$$h_{11}(t) = x(t) - m_{11}(t) \tag{3}$$

Demodulation $a_{11}(t)$ to $h_{11}(t)$ is obtained:

$$s_{11}(t) = h_{11}(t)/a_{11}(t) \tag{4}$$

4. In this case, we need to determine whether $s_{11}(t)$ is a pure frequency modulation function (pure frequency modulation function has a constant amplitude of 1, and $-1 \le s_{11}(t) \le 1$. If a_{12} is the envelope estimation function of $s_{11}(t)$ function, then $a_{12}(t) = 1$); if it is not a pure frequency modulation function, then return to step (1) and repeat the above iterative process for $s_{11}(t)$ until a pure frequency modulation signal $s_{1n}(t)$ is obtained, then:

$$\begin{aligned} h_{11}(t) &= x(t) - m_{11}(t) \\ h_{12}(t) &= s_{11}(t) - m_{12}(t) \\ &\vdots \\ h_{1n}(t) &= s_{1(n-1)}(t) - m_{1n}(t) \end{aligned} \tag{5}$$

5. Multiply all the local envelope functions generated in the whole iteration process to get the envelope signal $a_1(t)$:

$$a_1(t) = a_{11}(t)a_{12}(t)\cdots a_{1n}(t) = \prod_{q=1}^{n} a_{1q}(t) \tag{6}$$

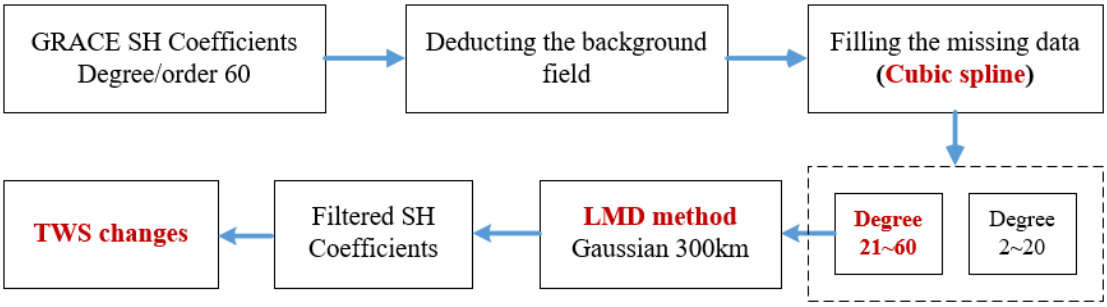

Fig. 1 The flowchart of filtering processing.

6. The first PF (Product Function) component of the original signal is the product of envelope signal $a_1(t)$ and pure FM (Frequency Modulation) signal $s_{1n}(t)$:

$$PF_1(t) = a_1(t)s_{1n}(t) \tag{7}$$

7. Component $PF_1(t)$ is separated from the original time series $x(t)$, and the new series $u_1(t)$ is used as a new original series. Steps (1) to (7) are repeated and repeated for k times until $u_k(t)$ is a monotone function.

$$\begin{aligned} u_1(t) &= x(t) - PF_1(t) \\ u_2(t) &= u_1(t) - PF_2(t) \\ &\vdots \\ u_k(t) &= u_{k-1}(t) - PF_k(t) \end{aligned} \tag{8}$$

8. After decomposition of many iterations, the original time series is finally decomposed into the form of the sum of k PF components and a margin $u_k(t)$, i.e.

$$x(t) = \sum_{p=1}^{k} PF_p(t) + u_k(t) \tag{9}$$

2.2. EXTRACTING THE GEOPHYSICAL SIGNALS FROM NOISY GRACE SH SOLUTIONS BY LMD

Based on the research of the GRACE SH models that noise is mainly existed in after 20 degrees (Yi and Sneeuw, 2022), for this reason here in this study we split the GRACE SH models into two parts, the part of lower 20 degree which do not filtering and higher 20 degree part which do filtering and the strategy is same as Yi and Sneeuw (2022). Before filtering we deduct background field of whole studying period of 2002 April to 2016 August. Each SH coefficient series can be divided into several PF components by LMD approach, and then determine the signal components by power spectrum analysis to reconstruct the signals. Similar to EMD, the PF components are arranged from high to low frequency, here we select the PF components whose period larger than 0.8 to reconstruct signal for the d/o 21~60 SH coefficients, which are decided through experimental comparisons. Since simply using LMD approach is not enough to remove strip errors accurately, therefore 300 km Gaussian smoothing are adopted together with LMD. The specific flowchart is shown in Figure 1.

With the GRACE SH time series filtered by LMD and EMD approaches, the global mass changes in terms of the equivalent water height (EWH) are computed as follows (Wahr et al., 1998),

$$\begin{aligned} \Delta h(\varphi,\lambda) = \frac{a\rho_{\text{ave}}}{3\rho_{\text{w}}} \sum_{l=0}^{\infty}\sum_{m=0}^{l} \bar{P}_{lm}(\sin\varphi)\frac{2l+1}{1+k_l}\cdot \\ \cdot(\Delta\bar{C}_{lm}\cos m\lambda + \Delta\bar{S}_{lm}\sin m\lambda) \end{aligned} \tag{10}$$

where a is the averaged Earth radius, ρ_{ave} is the mean Earth density, ρ_{w} is the water density, φ and λ are the latitude and longitude, respectively, $\bar{P}_{lm}(\sin\varphi)$ is the fully normalized associated Legendre function with degree l and order m, k_l is the load Love number of degree l, $\Delta\bar{C}_{lm}$ and $\Delta\bar{S}_{lm}$ are the SH coefficients reconstructed by LMD and EMD.

2.3. ADOPTED DATASETS

We adopt the SH coefficients models (truncated at maximum degree and order 60) provided by Center Space Research (CSR) covering the period from April 2002 to August 2016, with 17 missing months data. Besides, we add the degree-1 back and replace $C_{2,0}$ coefficients with the GRACE TN13 (Landerer, 2019) and SLR products (Loomis et al., 2020), correct the GIA effect with ICE6G-D model (Peltier et al., 2018). Noting that the missing data are filled using the cubic spline interpolation method (Guo et al., 2014).

Besides, hydrological models have been commonly used to validate the gravity field variation caused by the variations of soil moisture, near-surface air temperature, accumulated snow and other hydrological components over the land regions (Wang et al., 2021). Here in this study we adopt the monthly 1◦×1◦ GLDAS Noah models (https://daac.gsfc.nasa.gov/datasets?keywords=Noah), whose related parameters can be seen in the website https://daac.gsfc.nasa.gov.

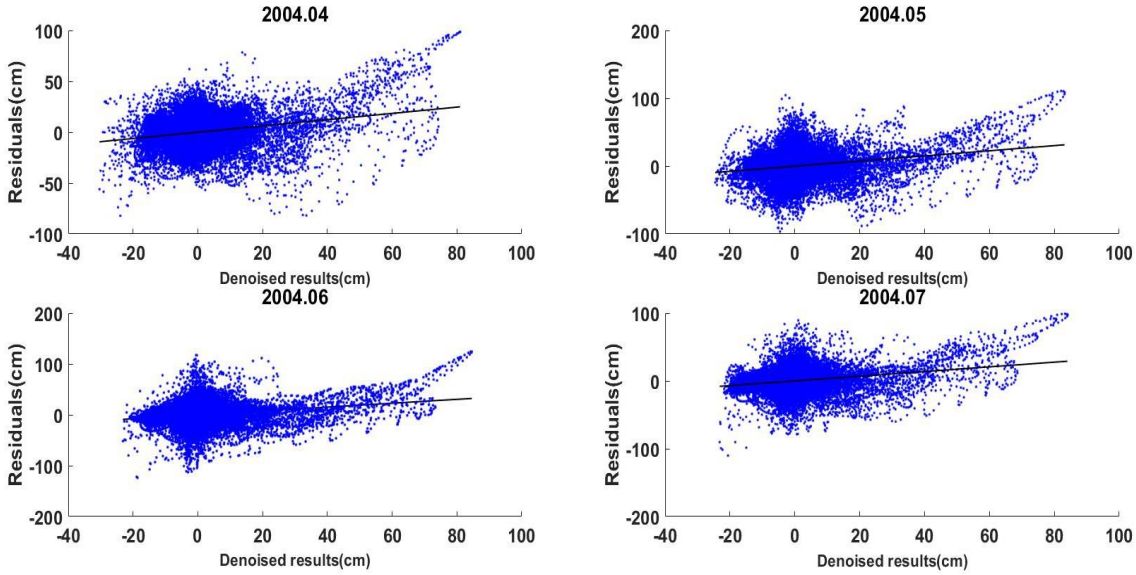

Fig. 2 The scatter plots of EWH for LMD from April to July 2004.

Table 1 Pearson correlation coefficient of four months in 2004.

Index	Pearson correlation coefficient		R^2	
	EMD	LMD	EMD	LMD
2004.04	0.2351	0.2144	0.0553	0.0460
2004.05	0.2248	0.1988	0.0505	0.0395
2004.06	0.2243	0.1955	0.0503	0.0382
2004.07	0.2199	0.1990	0.0484	0.0396

3. RESULTS AND ANALYSIS

3.1. THE CORRELATION ANALYSIS BETWEEN THE EXTRACTED GEOPHYSICAL SIGNAL AND NOISE

Normally assuming that the GRACE SH model contains additive noise (Eom et al., 2017; Pu et al., 2022), and the correlation between the signal and noise may not be very strong (Yang et al., 2022). To test the efficiency of LMD for extracting geophysical signals form noisy GRACE solutions, the global mass changes $\Delta h(\varphi,\lambda)$ in terms of the equivalent water height (EWH) ($1^\circ \times 1^\circ$ grids) are computed with the filtered GRACE SH time series by LMD and EMD based on Equation (10) (Wahr et al., 1998). At the same time, the filtered term $\Delta e(\varphi,\lambda)$ (noise) can also be obtained. Then we use three indexes including the scatter plots, Pearson correlation coefficient and R^2 (Square of the Pearson correlation coefficient) to analyze the correlation between the extracted gridded mass change signals and noise. No obvious patterns and smaller Pearson correlation coefficient indicate that the better filtering efficiency. The scatter plots of EWH in April, May, June and July 2004 are shown in Figure 2. It can be found that there are no apparent patterns between $\Delta h(\varphi,\lambda)$ and $\Delta e(\varphi,\lambda)$ among the selected four months, indicating that LMD can divide the signal and noise more reliably and accurately to some extent. The Pearson correlation coefficient and R^2 of LMD and EMD approaches are presented in Table 1.

As shown in Table 1, the Pearson correlation coefficients of LMD in three months are lower than 0.20, only one month slightly more than 0.2 and smaller than those of EMD approach, indicating that LMD performs better than EMD in filtering the noise, however there still exist relative weak correlations between the extracted geophysical signal and noise, may mainly due to the inaccurately separation between the signal and noise component. Besides, we further compute the square of the Pearson correlation coefficient, which draw the similar conclusion to that from Pearson correlation coefficients. Therefore, to better validate the performances of LMD in extracting the geophysical signals with respect to EMD approach, we will analyze the global mass changes in next sections.

3.2. THE COMPARISONS OF GLOBAL MASS CHANGE DERIVED FROM GRACE DATA

The global mass changes extracted by LMD and EMD approaches in September 2004 and March 2015 are shown in Figure 3. It is clearly to find that LMD can better filter out the noise than EMD with less remained noise. Considering the remaining noise, we adopted similar processing strategy to Shen et al. (2022) by applying 300 km Gaussian smoothing. To quantitatively evaluate the filtering efficiency of LMD

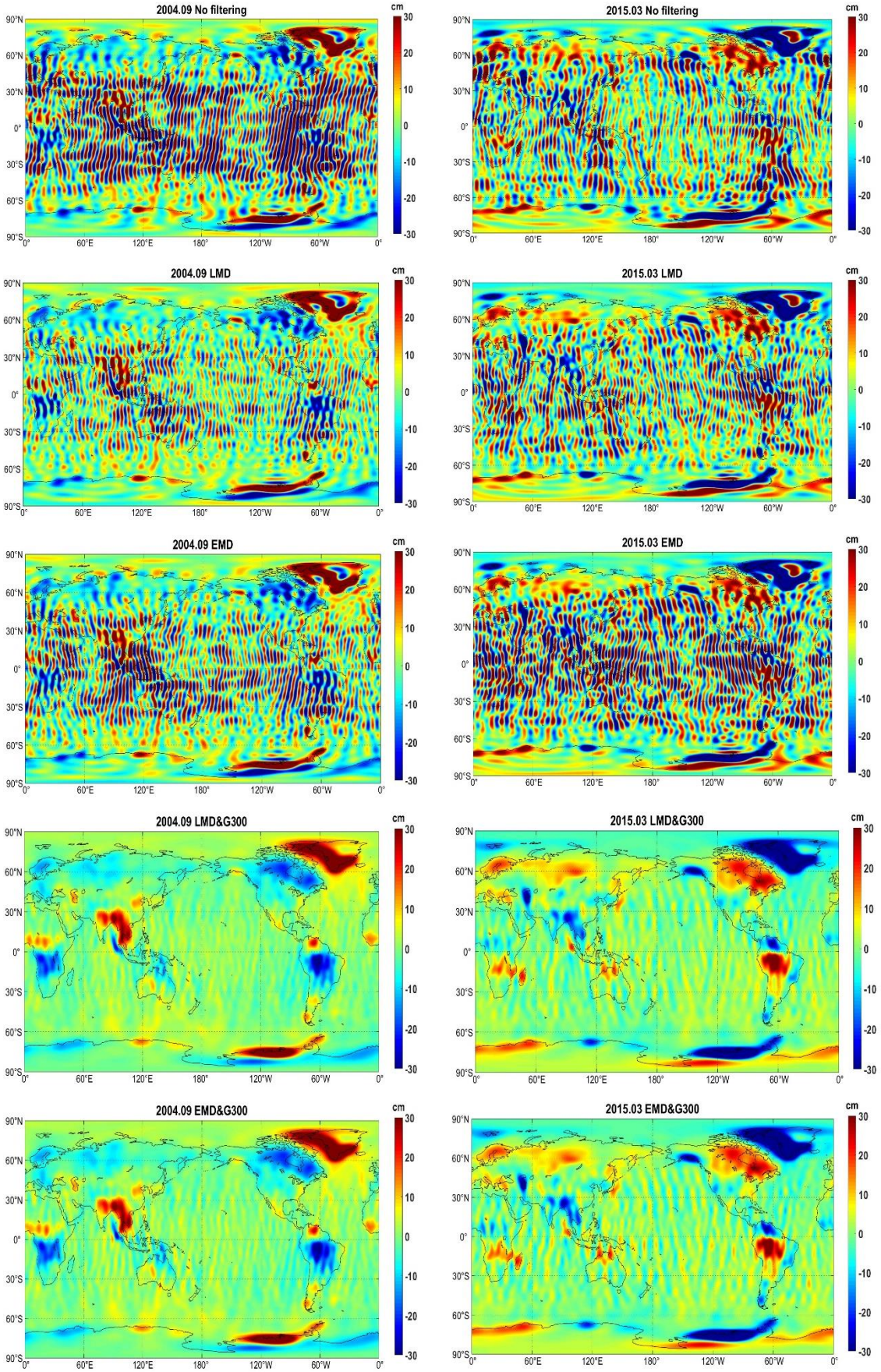

Fig. 3 Global mass change comparisons of LMD and EMD in September 2004 and March 2015.

Table 2 The RMS_ratios in September 2004 and March 2015.

Index	EMD	LMD	EMD&G300	LMD&G300
2004.09	1.4496	1.6482	3.3598	3.5419
2015.03	1.4124	1.6728	3.1871	3.5849

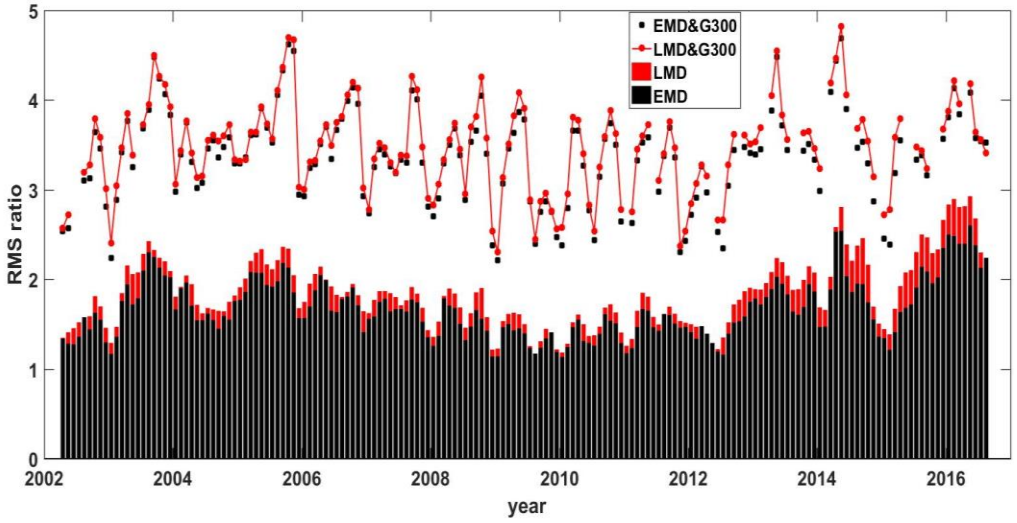

Fig. 4 The RMS_ratios of all available months over period April 2002 to August 2016.

and EMD, we computed the latitude weighted the ratio of RMS between land and oceans (Chen et al., 2006). To reduce the leakage of signals from land, a 300-km buffer zone is adopted.

$$RMS\_ratio = \frac{RMS(MASS_{land} + Err)}{RMS(MASS_{ocean} + Err)}, \quad (11)$$

where $MASS_{land}$ and $MASS_{ocean}$ represent the signals over lands and oceans, respectively, Err is the noise.

The corresponding RMS_ratios are presented in Table 2. The RMS ratio of LMD in September 2004 and March 2015 was 1.6482 and 1.6728, and 1.4496 and 1.4124 for EMD, respectively. After applying 300 km Gaussian smoothing (G300), the RMS_ratios of LMD, and EMD are increased. The RMS_ratios of LMD are all higher than EMD approach regardless of applying Gaussian smoothing or not, indicating that the advantage of LMD in extracting the geophysical signals with respect to EMD.

Figure 4 shows all the RMS_ratios of 156 available months of four adopted filtering methods. The mean RMS_ratios of LMD and EMD are 1.8329 and 1.6729, respectively. After 300 km Gaussian smoothing, the mean RMS_ratios are increased to 3.4458 and 3.3302, respectively. The relative improvements of the mean RMS_ratio of LMD with respect to EMD is 9.56%, after adopting the 300 km Gaussian smoothing, the relative improvements are 3.47 %, may mainly due to that 300 km Gaussian smoothing will weaken signals and produce additional signal leakage (Shen et al., 2021). In all, it is reasonable to conclude that LMD can extract geophysical signals and eliminate noise more efficiently than EMD approach.

3.3. TWS CHANGE COMPARISON WITH THE GLDAS NOAH MODEL OVER 25 GLOBAL RIVER BASINS

In section 3.2, we have analyzed and compared the global mass changes of LMD and EMD, and find that LMD can obtain higher RMS_ratios than EMD, which draw the conclusion that LMD can better filter out the noise. To detailed validate the signal extraction ability of LMD, here in this section we will adopt the GLDAS Noah model as reference signals. Since the GLDAS Noah model does not include groundwater changes, which, unlike the GRACE solution, are usually small over the basin, we eliminate their effects by subtracting the corresponding average and then obtaining the corresponding difference (Wang et al., 2021). The latitude weighted root mean squared errors (RMSE) are calculated as follows:

$$RMSE(\Omega) = \sqrt{\frac{\sum_{\forall i \in \Omega} (\Delta v_i^{\,2} . \cos\varphi_i)}{\sum_{\forall i \in \Omega} \cos\varphi_i}} \quad (12)$$

where Δv_i represents the differences between the GLDAS signals and the reconstructed signals by LMD and EMD, φ_i is the corresponding latitude, Ω represents a spatial range and can be global or regional. And all grids within Ω are summed based on their area weights reflected by latitudes.

Here we take three river basins Limpopo, Wisla and Mississippi rivers basins as example. The correlation coefficients and RMSEs of all EWH grid data of LMD and EMD combined with Gaussian smoothing 300km relative to the GLDAS Noah model over three river basins are respectively presented in Figures 5 and 6. In Figures 5 and 6, it is clearly to see

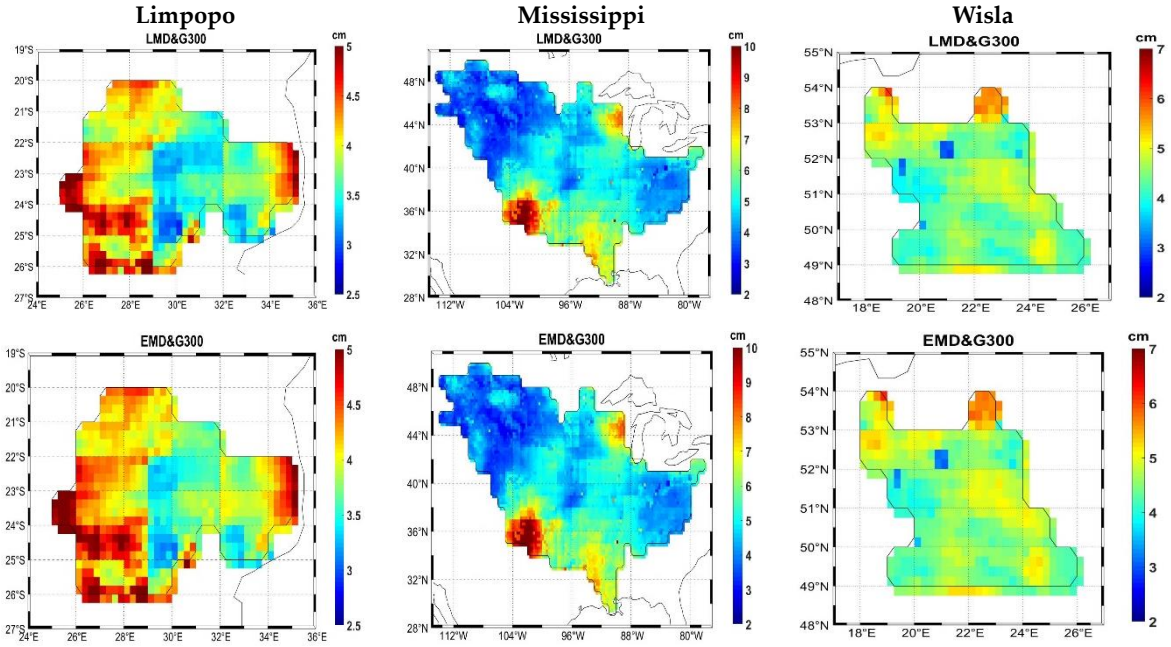

Fig. 5 RMSEs of using LMD and EMD methods relative to the GLDAS Noah models over three river basins.

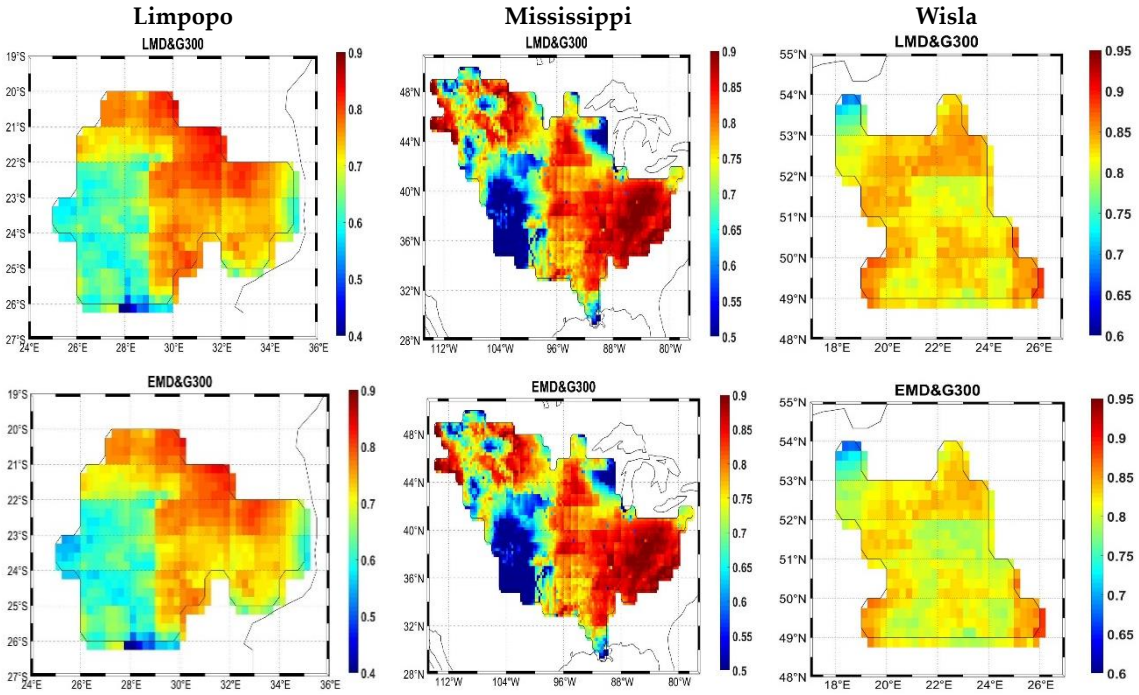

Fig. 6 Pearson correlation coefficients of using LMD and EMD methods relative to the GLDAS Noah model over three river basins.

that the RMSEs of the LMD&G300 over three river basins are similar to those of EMD&G300 approach just with slight smaller values and higher correlation coefficients.

To quantitatively evaluate the extracted TWS change signals of LMD and EMD with respect to GLDAS models, Figure 7 shows the computed TWS change series and absolute differences with respect to GLDAS Noah models over three river basins. The RMSEs and correlation coefficients are computed and presented in Table 3. The RMSEs of LMD are all smaller than those of EMD approach, likewise the higher Pearson correlation coefficients over three river basins. Through the above results, we can draw the conclusion that after the combination filter of the LMD is closer to the GLDAS Noah models in three river basins.

Finally, we selected 25 major river basins around the world, whose spatial distributions are shown in Figure 8. The corresponding statistics results are summarized in Table 4, which including the mean latitude weighted RMSEs and the corresponding

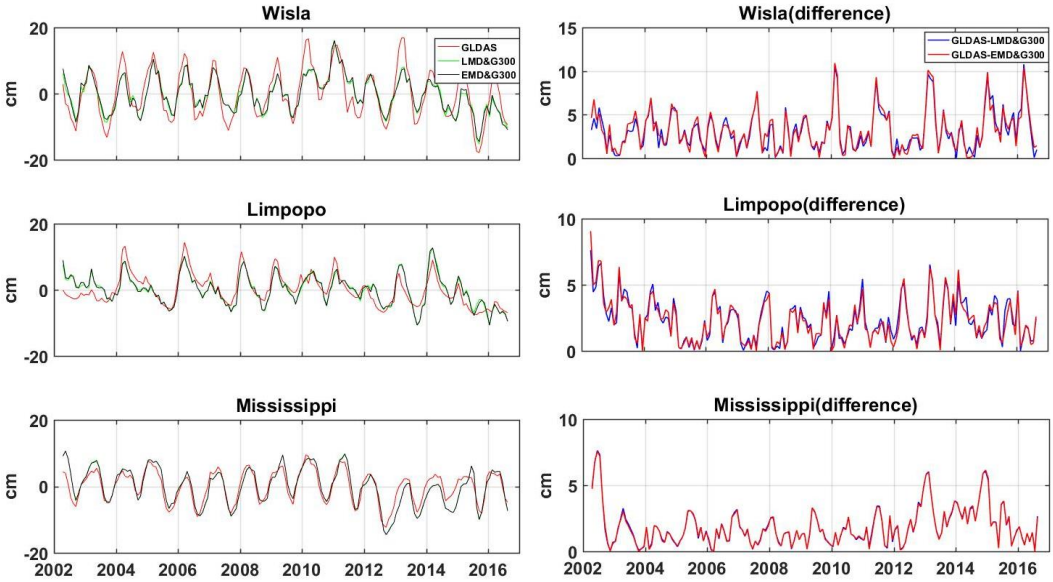

Fig. 7 The TWS change series and absolute differences between TWS change series and GLDAS Noah models in three river basins.

Table 3 The RMSEs and Pearson correlation coefficients of LMD&G300 and EMD&G300 with respect to GLDAS Noah models.

Index	RMSE/cm		Pearson correlation coefficients	
	LMD&G300	EMD&G300	LMD&G300	EMD&G300
Wisla	4.5031	4.6118	0.8256	0.8131
Limpopo	3.9282	4.0512	0.7034	0.6925
Mississippi	4.9373	4.9665	0.7310	0.7271

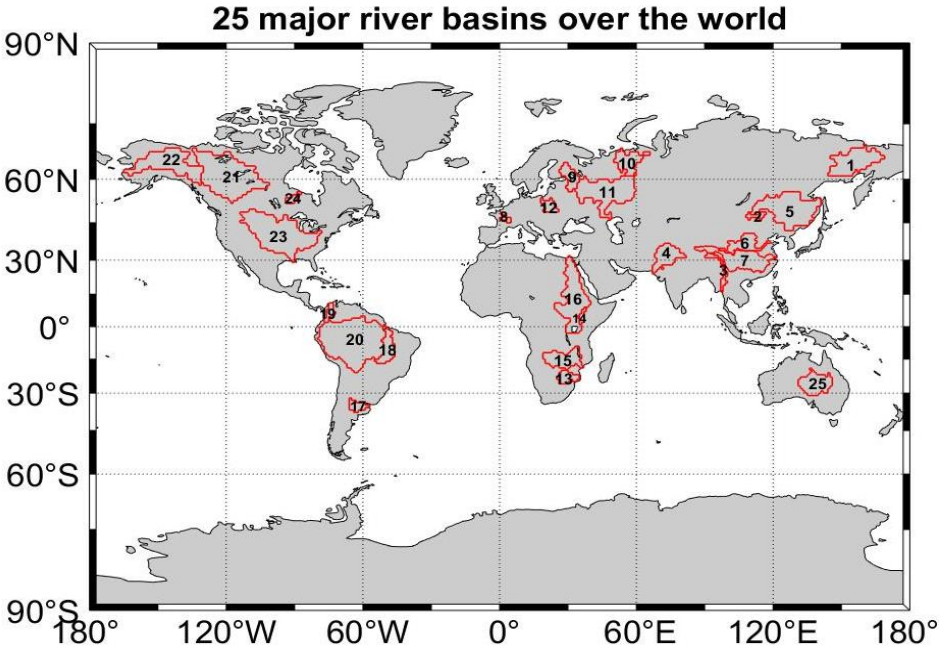

Asia
1 Kolyma
2 Kerulen
3 Salween
4 Indus
5 Amur
6 Yellow River
7 Yangtze

Europe
8 Loire
9 Neva
10 Pechora
11 Volga
12 Wisla

Africa
13 Limpopo
14 Lake Rudolf
15 Zambezi
16 Nile

South America
17 Salado
18 Tocantins
19 Magdalena
20 Amazon

North America
21 Mackenzie
22 Yukon
23 Mississippi
24 Severn

Oceania
25 Lake Eyre

Fig. 8 The selected 25 major rivers basins around the world.

Table 4 The mean RMSEs of LMD and EMD with respect to GLDAS Noah models and corresponding relative improvement percentages (IMP) for 25 major river basins.

Index	ID	RMSE (cm)		IMP (%)
		LMD&G300	EMD&G300	
Kolyma	1	4.9185	5.0335	2.28
Kerulen	2	1.9747	2.0249	2.48
Salween	3	5.4269	5.5493	2.21
Indus	4	6.2589	6.3238	1.03
Amur	5	4.4023	4.4170	0.33
Yellow river	6	3.7236	3.7368	0.35
Yangtze	7	4.7199	4.8127	1.93
Loire	8	5.2868	5.3154	0.54
Neva	9	7.6997	7.7302	0.40
Pechora	10	6.3423	6.3514	0.14
Volga	11	6.2462	6.2807	0.55
Wisla	12	4.0320	4.1413	2.64
Limpopo	13	3.7292	3.8278	2.58
Lake Rudolf	14	6.1948	6.2270	0.52
Zambezi	15	8.7909	8.8653	0.84
Nile	16	5.3328	5.4256	1.71
Salado	17	5.7483	5.7512	0.06
Tocantins	18	9.6463	9.8051	1.62
Magdalena	19	5.5472	5.6394	1.63
Amazon	20	12.2075	12.4049	1.59
Mackenzie	21	7.1362	7.1571	0.30
Yukon	22	10.2371	10.2445	0.07
Mississippi	23	4.9187	4.9540	0.72
Severn	24	8.4950	8.5160	0.16
Lake Eyre	25	3.4594	3.5856	3.52

relative improvement percentage (IMP) of 25 major river basins from April 2002 to August 2016. We can find that all RMSEs of 25 river basins of LMD are less than those of EMD approach. The corresponding IMPs of RMSE for LMD with respect to EMD range from 0.07 to 3.52. Based on the above analysis, the extracted TWS signals by LMD are closer to those of GLDAS Noah models than EMD, therefore we can believe that LMD can more efficiently and accurately extract the geophysical signals and filtering the strong noise of GRACE SH solutions.

4. CONCLUSIONS

Strong noise drowns the geophysical signals in GRACE monthly SH coefficients solutions, which limits the study of TWS change over global main river basins. In this contribution, we firstly apply LMD for extracting the TWS change signals during the filtering procedure together with EMD approach. The computed scatter plots, Pearson correlation coefficient and R^2 (Square of the Pearson correlation coefficient) show that LMD can better divide the signal and noise with the smaller correlation coefficients and R^2 values. All RMS _ratios of LMD are higher than EMD regardless of applying the 300 km Gaussian smoothing or not, indicating that LMD outperforms EMD in filtering noise and extracting geophysical signals. Besides, through the comparisons with GLDAS Noah model in 25 major river basins around the world, it can be found that the mean latitude weighted RMSEs for LMD approach are all smaller than that of EMD, indicating that the extracted TWS change signals by LMD are closer to those of GLDAS Noah models. Therefore, we can conclude that LMD is better than EMD for extracting geophysical signals and filtering the noise from GRACE solutions.

ACKNOWLEDGMENT:

This work is mainly funded by the Natural Science Foundation of China (42064001, 42061077).

REFERENCES

Bettadpur, S.: 2012, Insights into the Earth System mass variability from CSR-RL05 GRACE gravity fields. EGU General Assembly 2012, Geophys. Res. Abstr., 14, 6409.

Chambers, D.P. and Bonnin J.A.: 2012, Evaluation of Release-05 GRACE time-variable gravity coefficients over the ocean. Ocean Sci., 8, 5, 859–868. DOI: 10.5194/os-8-859-2012

Chen, Q., Shen, Y., Kusche, J., Chen, W., Chen, T. and Zhang, X.: 2021, High-Resolution GRACE Monthly Spherical Harmonic Solutions. J. Geophys. Res., Solid Earth, 126, 1, e2019JB018892. DOI: 10.1029/2019JB018892

Chen, J., Wilson, C.R., Famiglietti, J.S. and Rodell, M.: 2007, Attenuation effect on seasonal basin-scale water storage changes from GRACE time-variable gravity. J. Geod., 81, 4, 237–245. DOI: 10.1007/s00190-006-0104-2

Chen, J., Wilson, C.R. and Seo, K.-W.: 2006, Optimized smoothing of Gravity Recovery and Climate Experiment (GRACE) time-variable gravity observations. J. Geophys. Res., Solid Earth, 111, B6. DOI: 10.1029/2005JB004064

Cheng, J., Yang, Yi. and Yang, Yu.: 2012, A rotating machinery fault diagnosis method based on local mean decomposition. Digit. Signal Process., 22, 2, 356–366. DOI: 10.1016/j.dsp.2011.09.008

Davis, J.L., Tamisiea, M.E., Elosegui, P. et al.: 2008, Statistical filtering approach for Gravity Recovery and Climate Experiment (GRACE) gravity data. J. Geophys. Res., Solid Earth, 113, B4. DOI: 10.1029/2007JB005043

Duan, X.J., Guo, J.-Y., Shum, C.K. et al.: 2009, On the postprocessing removal of correlated errors in GRACE temporal gravity field solutions. J. Geod., 83, 11, 1095–1106. DOI: 10.1007/s00190-009-0327-0

Eom, J., Seo, K.-W.: and Ryu, D.: 2017, Estimation of Amazon River discharge based on EOF analysis of GRACE gravity data. Remote Sens. Environ., 191, 55–66. DOI: 10.1016/j.rse.2017.01.011

Guo, J., Mu, D., Liu, X.,…, Dai H.: 2014, Equivalent water height extracted from GRACE gravity field model with robust independent component analysis. Acta Geophys., 62, 4, 953–972. DOI: 10.2478/s11600-014-0210-0

Han, S.C., Shum, C.K., Jekeli, C.,…, Seo, K.-W.: 2005, Non-isotropic filtering of GRACE temporal gravity for geophysical signal enhancement. Geophys. J. Int., 163, 1, 18–25. DOI: 10.1111/j.1365-246X.2005.02756.x

Huan, C., Wang, F. and Zhou, S.: 2022, Empirical mode decomposition for post-processing the GRACE monthly gravity field models. Acta Geodyn. Geomater., 19, 4 (208), 281–290: DOI: 10.13168/AGG.2022.0013

Huan, C., Wang, F. and Zhou, S. and Qiu, X.: 2023, Filtering GRACE temporal gravity field solutions using ensemble empirical mode decomposition approach. Front. Earth Sci., 11, 1132862. DOI: 10.3389/feart.2023.1132862

Klees, R., Revtova, E.A., Gunter, B.C., Ditmar, P., Oudman, E., Winsemius, H.C. and Savenije, H.H.G.: 2008, The design of an optimal filter for monthly GRACE gravity models. Geophysi. J. Int., 175, 2, 417–432. DOI**:** 10.1111/j.1365-246X.2008.03922.x

Landerer, F.: 2019, Monthly estimates of degree-1 (geocenter) gravity coefficients, generated from GRACE (04-2002–06/2017) and GRACE-FO (06/2018 onward) RL06 solutions. GRACE Technical Note 13, The GRACE Project. NASA Jet Propulsion Laboratory.

Loomis, B.D., Rachlin, K.E., Wiese, D.N., …, Luthcke, S.B.: 2020, Replacing GRACE/GRACE-FO with satellite laser ranging: Impacts on Antarctic Ice Sheet mass change. Geophys. Res. Lett., 47, 3, e2019GL085488. DOI: 10.1029/2019GL085488

Mu, D., Guo J., Sun, Z. and Kong, Q.: 2014, Equivalent water height of GRACE gravity field model based on principal component analysis. Progress in Geophysics, 29, 4, 1512-1517. DOI: 10.6038/pg20140405

Peltier, W., Argus D.F. and Drummond, R.: 2018, Comment on an assessment of the ICE-6G_C (VM5a) glacial isostatic adjustment model by Purcell et al. J. Geophys. Res., Solid Earth, 123, 2, 2019–2028. DOI: 10.1002/2016JB013844

Pu, L., Fan, D., You, W. …, Zhongshan, J.: 2022, Extracting terrestrial water storage signals from GRACE solutions in the Amazon Basin using an iterative filtering approach. Remote Sens. Lett., 13, 1, 14–23. DOI: 10.1080/2150704X.2021.1981557

Qiu, X., Wang, F., Zhou, S. and Zou S.: 2020, Application of local mean decomposition and singular value decomposition in noise reduction of GNSS station coordinate time series signal. Bulletin of Surveying and Mapping, 0, 5, 85–89. DOI: 10.13474/j.cnki.11-2246.2020.0151

Sasgen, I.., Martinec, Z. and Fleming, K.M.: 2007, Wiener optimal combination and evaluation of the Gravity Recovery and Climate Experiment (GRACE) gravity fields over Antarctica. J. Geophys. Res., Solid Earth, 112, B4. DOI: 10.1029/2006JB004605

Shen, Y., Wang, F. and Chen, Q.: 2021, Weighted multichannel singular spectrum analysis for post-processing GRACE monthly gravity field models by considering the formal errors. Geophys. J. Int., 226, 3, 1997–2010. DOI: 10.1093/gji/ggab199

Smith, J. S.: 2005, The local mean decomposition and its application to EEG perception data. J. R. Soc. Interface, 2, 5, 443–454. DOI: 10.1098/rsif.2005.0058

Sun, J., Xiao, Q., Wen, J. and Zhang, Y.: 2016, Natural gas pipeline leak aperture identification and location based on local mean decomposition analysis. Measurement, 79, 147–157. DOI: 10.1016/j.measurement.2015.10.015

Swenson, S. C. and Wahr, J.M.: 2011, Estimating signal loss in regularized GRACE gravity field solutions. Geophys. J. Int., 185, 2, 693–702. DOI: 10.1111/j.1365-246X.2011.04977.x

Wahr, J., Molenaar, M. and Bryan F.: 1998, Time variability of the Earth's gravity field: Hydrological and oceanic effects and their possible detection using GRACE. J. Geophys. Res., Solid Earth, 103, B12, 30205–30229. DOI: 10.1029/98JB02844

Wang, F., Shen, Y. Chen, T. …, Li, W.: 2020, Improved multichannel singular spectrum analysis for post-processing GRACE monthly gravity field models. Geophys. J. Int., 232, 2, 825–839. DOI: 10.1093/gji/ggaa339

Wang, F., Shen, Y. and Uni, T.: 2021, Bridging the gap between GRACE and GRACE follow-on monthly gravity field solutions using improved multichannel singular spectrum analysis. J. Hydrol., 594, 125972. DOI: 10.1016/j.jhydrol.2021.125972

Wang, Y., He, Z. and Zi, Y.: 2010, A comparative study on the local mean decomposition and empirical mode decomposition and their applications to rotating machinery health diagnosis. J. Vib. Acoust., 132, 2. DOI: 10.1115/1.4000770

Wouters, B., Bonin, J.A., Chambers, D.P., , Wahr, J.: 2014, GRACE, time-varying gravity, Earth system dynamics and climate change. Rep. Prog. Phys., 77, 11, 116801. DOI: 10.1088/0034-4885/77/11/116801

Yang, T., Yu, H. and Wang, Y.: 2022, An efficient low-pass-filtering algorithm to de-noise global GRACE data. Remote Sens. Environ., 283, 113303. DOI: 10.1016/j.rse.2022.113303

Yi, S. and Sneeuw. N.: 2022, A novel spatial filter to reduce north–south striping noise in GRACE spherical harmonic coefficients. J. Geod., 96, 4, 1–17. DOI: 10.1007/s00190-022-01614-z

Zhang, Z., Chao, B.F., Lu, Y. and Hsu, H.-T.: 2009, An effective filtering for GRACE time-variable gravity: Fan filter. Geophys. Res. Lett., 36, 17. DOI: 10.1029/2009GL039459

Zhong, B., Li, X., Chen, J. and Li, Q.: 2023, WHU-GRACE-GPD01s: 2023: A series of constrained monthly gravity field solutions derived from GRACE-based geopotential differences. Earth Space Sci., 10, 4, e2022EA002699. DOI: 10.1029/2022EA002699